

CALCULATE THE EFFICIENCY OF GAMMA-RAY DETECTORS FOR INVERTED WELL BEAKER SOURCES USING AN ANALYTICAL EFFICIENCY TRANSFER PRINCIPLE

Different sources efficiency measurements and the construction of the corresponding calibration curve are usually carried out in gamma-ray spectrometry to calculate the unknown activity for different sources in the same geometry or in order to facilitate the efficiency computation of different source geometries by the use of the efficiency transfer method. In this work, the Full Energy Peak Efficiency value (FEPE) of HPGe detector has been calculated using axial inverted well beaker sources of different dimensions by an analytical approach of effective solid angle ratio. Calculation taking into account the source self attenuation effect, this approach is based on the direct mathematical method. In the experiments gamma aqueous sources containing ^{152}Eu radionuclide's covering the energy range from 121 to 1408 keV were used. By comparison, the theoretical and experimental full-energy peak efficiency values are in good agreement.

Key words: HPGe detector, Full Energy Peak Efficiency (FEPE), Efficiency Transfer.

Introduction

The efficiency transfer (ET) method was introduced by Moens et al. in 1981 and has since attained popularity as a means of calculating the full-energy-peak efficiencies (FEPE) for measurements in gamma-ray spectrometry, instead of directly comparing the measured sample with a standard of the same size, composition, density and radionuclide contents (Gilmore, 2008). The method works by computing with the help of a suitable detector model efficiencies for the measured sample and for the standard. A ratio of these two efficiencies is then multiplied with the experimentally determined FEPE value of the standard to arrive at the corresponding efficiency of the measured sample.

The main advantage of the efficiency transfer (ET) approach with a point calibration source located at a sufficient distance from the detector is that one may neglect coincidence summing effects and obtain a coincidence free efficiency curve. The use of point sources is standard in the determination of the gamma-ray efficiency for detectors.

In this work we examine the applicability of the efficiency transfer method (ET) for computation the efficiency of a hyper pure germanium (HPGe) by using different inverted well beaker aqueous sources containing ^{152}Eu , based on reference point source located at several distances $P_4=20$ cm, $P_5=25$ cm and $P_6=30$ cm from the detector surface in order to get the effective solid angle which required to apply this Method

and the compares the theoretical result with the measured one.

Mathematical viewpoint

The basic relationship which makes it possible to express the efficiency as a function of the reference efficiency, known at the same energy, E :

$$\varepsilon(E, P) = \varepsilon(E, P_o) \frac{\Omega_{eff}(P)}{\Omega_{eff}(P_o)} \quad (1)$$

Where, $\varepsilon(E, P_o)$ & $\varepsilon(E, P)$ are the efficiencies, at energy, E , of a point source located at positions, P_o & P respectively and are given by:

$$\varepsilon(E, P_o) = \varepsilon_i(E) \cdot \Omega_{eff}(P_o), \quad (2)$$

$$\varepsilon(E, P) = \varepsilon_i(E) \cdot \Omega_{eff}(P). \quad (3)$$

Where, $\varepsilon_i(E)$, represents the intrinsic efficiency of the detector for energy, E , and, $\Omega_{eff}(P_o)$ is the effective solid angle subtended by point, P_o , and the active surface of the detector, this geometrical factor must include absorbing factors, taking into account the attenuation effects of the materials between the source and the active part of the source matrix, Piton et al. [7].

In general by knowing the source-detector geometry, we can compute the detector efficiency for different shapes using the principle of efficiency transfer by computing the relevant solid angle and absorbing factors, Jovanovic et al. [8]. Selim and co-workers using the spherical coordinate system derived direct analytical elliptic integrals to calculate the detector efficiencies

(total and full-energy peak) for any source-detector configuration, Badawi [9]

The pure solid angle, (Ω), subtended by the detector at the source point has been given in Abbas [10], and it is defined as

$$\Omega = \int_{\theta} \int_{\varphi} \sin \theta d\varphi d\theta . \quad (4)$$

The effective solid angle is defined as:

$$\Omega_{eff} = \int_{\theta} \int_{\varphi} f_{att} \sin \theta d\varphi d\theta . \quad (5)$$

Where, f_{att} , factor determines the photon attenuation by all absorbers between source and detector and it is expressed as:

$$f_{att} = e^{-\sum_i \mu_i \delta_i} . \quad (6)$$

Where, μ_i , is the attenuation coefficient of the, i^{th} , absorber for a gamma-ray photon with energy, E_γ , and, δ_i , is the average gamma photon path length through the, i^{th} , absorber.

The location of an arbitrarily positioned axial point source is specified by, (h) where, h , is the source-detector distance see figure (1), and the polar, θ , and the azimuth, φ , angles at the point of entrance of the considered surface define the direction of the incidence of a gamma-ray photon.

Therefore the effective solid angle can be expressed as:

$$\Omega_{eff} = 2 \sum_{i=1}^{n=2} Y_i . \quad (7)$$

Where:

$$Y_1 = \int_0^{\theta_1} \int_0^{2\pi} f_{att} \sin \theta d\varphi d\theta , \quad Y_2 = \int_{\theta_1}^{\theta_2} \int_0^{2\pi} f_{att} \sin \theta d\varphi d\theta \quad (8)$$

The polar angles can be expressed as, Abbas [10]

$$\theta_1 = \tan^{-1} \left(\frac{R}{h+L} \right) \quad \& \quad \theta_2 = \tan^{-1} \left(\frac{R}{h} \right) . \quad (9)$$

The volumetric source can be treated as group of point sources which are uniformly distributed; each point source has the effective solid angle, $\Omega_{eff(Po\ int)}$, Nafee [11] as shown in equation (10).

$$\Omega_{eff(Cyl)} = \frac{\int f_{att} \cdot \Omega_{eff(Po\ int)} dV}{V} . \quad (10)$$

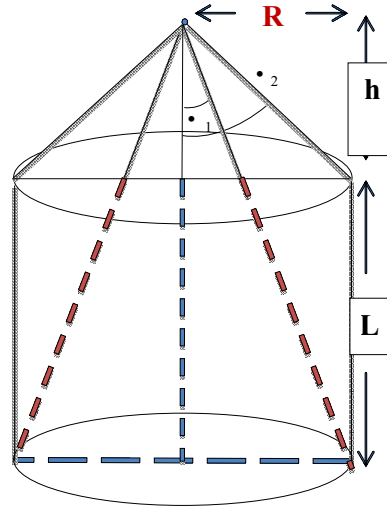


Figure (1) an axial point source with cylindrical detector

To calculate the effective solid angle of the detector using a radioactive cylindrical source of dimensions larger than the detector choose an arbitrary element of volume, dV , at lateral distance, c , from the detector axis and making an angle, θ , with the detector's major axis, h , is the source-detector separation, this element of volume can be expressed in the polar coordinates by: $dV = \rho d\rho d\alpha dh$.

The equation (10) will be:

$$\Omega_{eff(Cyl)} = \frac{\int \int \int f_{att} \cdot \Omega_{eff(Po\ int)} \rho d\rho d\alpha dh}{h \alpha \rho V} . \quad (11)$$

In order to measure the efficiency of the detector for the used inverted well beaker (Marinelli beaker), we divide the inverted well source into five parts with volumes, V_1, V_2, V_3, V_4 , and, V_5 , as shown in figure (2). The volume V_1 acts as a solid cylinder with height, L_1 , and radius, R , while the volumes, V_2, V_3, V_4 and, V_5 , acts as a thick cylindrical ring with height, L_1, h_o, L , and, L_2 , respectively, with inner radius, S_1 , and outer radius, S_2 .

The effective solid angle of the detector, Ω_{Mar} , in case of using an inverted well source (Abbas, 2000):

$$\Omega_{Mar} = \frac{\sum_{i=1}^5 \Omega_i \cdot V_i}{\sum_{i=1}^5 V_i} . \quad (12)$$

Where the solid angle of each part of the Marinelli beaker, $\Omega_1, \Omega_2, \Omega_3, \Omega_4$, and, Ω_5 , are for the volumes, V_1, V_2, V_3, V_4 , and, V_5 , respectively, are given:

$$\Omega_1 = \frac{1}{\pi R^2 L_1} \int_{h_o}^{h_o+L_1} \int_0^{2\pi} \int_0^R S_f \cdot \Omega_{\text{point}(\rho < R)} \rho d\rho d\alpha dh$$

$$\Omega_2 = \frac{1}{r(S_2^2 - R^2) L_1} \int_{h_o}^{h_o+L_1} \int_0^{2\pi} \int_0^{S_2} S_f \cdot \Omega_{\text{point}(\rho \geq R)} \rho d\rho d\alpha dh$$

$$\Omega_3 = \frac{1}{r(S_2^2 - S_1^2) h_o} \int_0^{h_o} \int_0^{2\pi} \int_{S_1}^{S_2} S_f \cdot \Omega_{\text{point}(\rho \geq R)} \rho d\rho d\alpha dh$$

$$\Omega_4 = \frac{1}{r(S_2^2 - S_1^2) L} \int_0^L \int_0^{2\pi} \int_{S_1}^{S_2} S_f \cdot \Omega_{\text{point}(\rho \geq R)} \rho d\rho d\alpha dh$$

$$\Omega_5 = \frac{1}{r(S_2^2 - S_1^2) L_2} \int_0^{L_2} \int_0^{2\pi} \int_{S_1}^{S_2} S_f \cdot \Omega_{\text{point}(\rho \geq R)} \rho d\rho d\alpha dh$$

To determine the absorption of photons through the inverted well source, there are two factors to be considered, the first is the self-absorption factor by the source medium, and the second one is the attenuation factor by the inverted well container material, dead layer and end-cap and the absorber between the source and the detector.

For the given inverted well source and photon energy, the self-absorption is a function of the path length of the photon in the source medium. Table (1) shows that there are two different allowed photon path lengths, d_s , (through

the source medium) corresponding to the main four cases of the photon traveling distances, d_1 , through the detector active medium. The path lengths d_1 & d_2 where, $\Omega_{\text{point}}, (\rho < R \text{ and } \rho \geq R)$ while the path lengths d_3 & d_4 where, $\Omega_{\text{point}}, (\rho \geq R)$, Badawi [9].

The attenuation of the inverted well containers (Marinelli beakers) of thickness, t_5 , the dead layer of thickness, t_1 , the end-cap with thickness, t_3 , and the absorber of thickness, t_4 , is a function of the photon path length through these materials. Table (1) shows the four different photon path lengths through inverted well container, dead layer, end-cap and absorber material ($\delta t_5, \delta t_1, \delta t_3$, and, δt_4 , respectively) corresponding to the main four cases of the photon traveling distances, d_1 , through the detector active medium, Badawi [9].

Table (1) The photon path lengths through the source-detector system, Badawi [9]

d	d_s			
d_1, d_2	$\frac{h-h_o}{\cos\theta}$			
d_3, d_4	$\frac{\rho \cos\phi + \Delta\sqrt{R^2 - \rho^2 \sin^2\phi} - S_o}{\sin\theta}$			
d	δt_5	δt_1	δt_3	δt_4
d_1, d_2	$\frac{t_5}{\cos\theta}$	$\frac{t_1}{\cos\theta}$	$\frac{t_3}{\cos\theta}$	$\frac{t_4}{\cos\theta}$
d_3, d_4	$\frac{t_5}{\sin\theta}$	$\frac{t_1}{\sin\theta}$	$\frac{t_3}{\sin\theta}$	$\frac{t_4}{\sin\theta}$

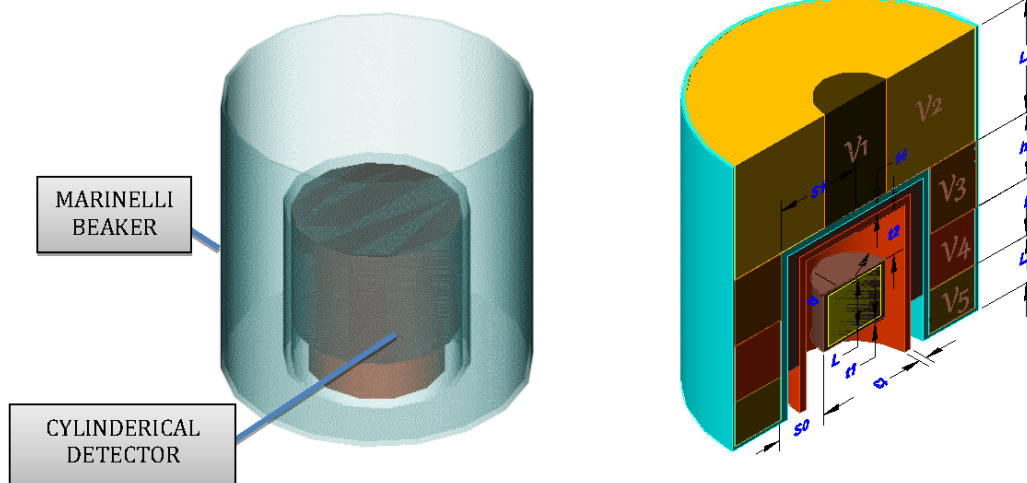


Figure 2 Inverted well beaker source with a cylindrical detector

Experimental setup

The p-type HPGe detector with a 15% relative efficiency was used for the experimental verification of the proposed method which its characteristics are shown in Table (2).

In the first step, the detector efficiency was determined experimentally, as a function of gamma-ray energies using ¹⁵²Eu point source (PTB), purchased from The Physikalisch-Technische Bundesanstalt (PTB) in Braunschweig and Berlin, which located at 20, 25, 30 cm from the face of a homemade Plexiglas holder (figure (3)) which placed directly on the detector entrance window as an absorber to avoid the effect of β- and x-rays and to protect the detector heads, so there is no correction was made for x-gamma coincidences, since in most cases the accompanying x-ray were soft enough to be absorbed completely before entering the detector. The source-detector separations start from 20 cm to neglect the coincidence summing correction.

Where the detector efficiency using different volumes inverted well beakers (Marinelli beakers), which placed directly on the detector end-cap, is also measured experimentally. The used inverted well beakers M1&M2 purchased from GA-MA & ASSOCIATES,INC company

and M3 purchased from Nuclear Technology Services,Inc. The angular correlation effects can be negligible for the low source-to-detector distance, Debertain, et al. [12]

The certificates give the sources activities and their uncertainties for all sources used are listed in table (4). The data sheet states values of half-lives, photon energies and photon emission probabilities per decay for the all radionuclides used in the calibration process are listed in table (4), which available from the National Nuclear Data Center Web Page or on the IAEA website. Also, the dimensions of the used inverted well beakers are given in table (5).

The spectrum acquired by winTMCA32 software made by ICx Technologies, were analyzed by (Genie 2000 data acquisition and analysis software) made by Canberra using its automatic peak search and peak area calculations, along with changes in the peak fit using the interactive peak fit interface when necessary to reduce the residuals and error in the peak area values. The live time, the run time and the start time for each spectrum were entered into the spreadsheets. These sheets were used to perform the calculations necessary to generate the experimental full energy peak efficiency (FEPE)

Table (2) Setup parameters with acquisition electronics specifications for HPGe detector

Manufacturer	Canberra Industries	Drawing
Serial Number	06089367	
Detector Model	GC1520	
Geometry	Closed end Coaxial	
Relative Efficiency (%)	15	
Photopeak – Compton ratio	40	
Voltage bias (V)	(+) 4500	
Crystal Model	7500SL	
Resolution (FWHM) at 133 keV	2.0 keV	
Shaping time (τ s)	4	
Preamplifier Model	2002CSL	
Amplifier Model	2026	
MCA	Multi port II	
VPS Model	3106D	
Detector type	HPGe (P- type)	
Shaping Model	Gaussian	
Mounting	Vertical	
Outer Electrode Thickness (mm)	0.5	
Inner Electrode Thickness (mm)	0.3x10 ⁻³	
Window Electrode Thickness (mm)	0.5	
Crystal Diameter (mm)	48	
Crystal Length (mm)	54.5	
Core hole Diameter (mm)	7.5	
Core hole Depth (mm)	37.5	

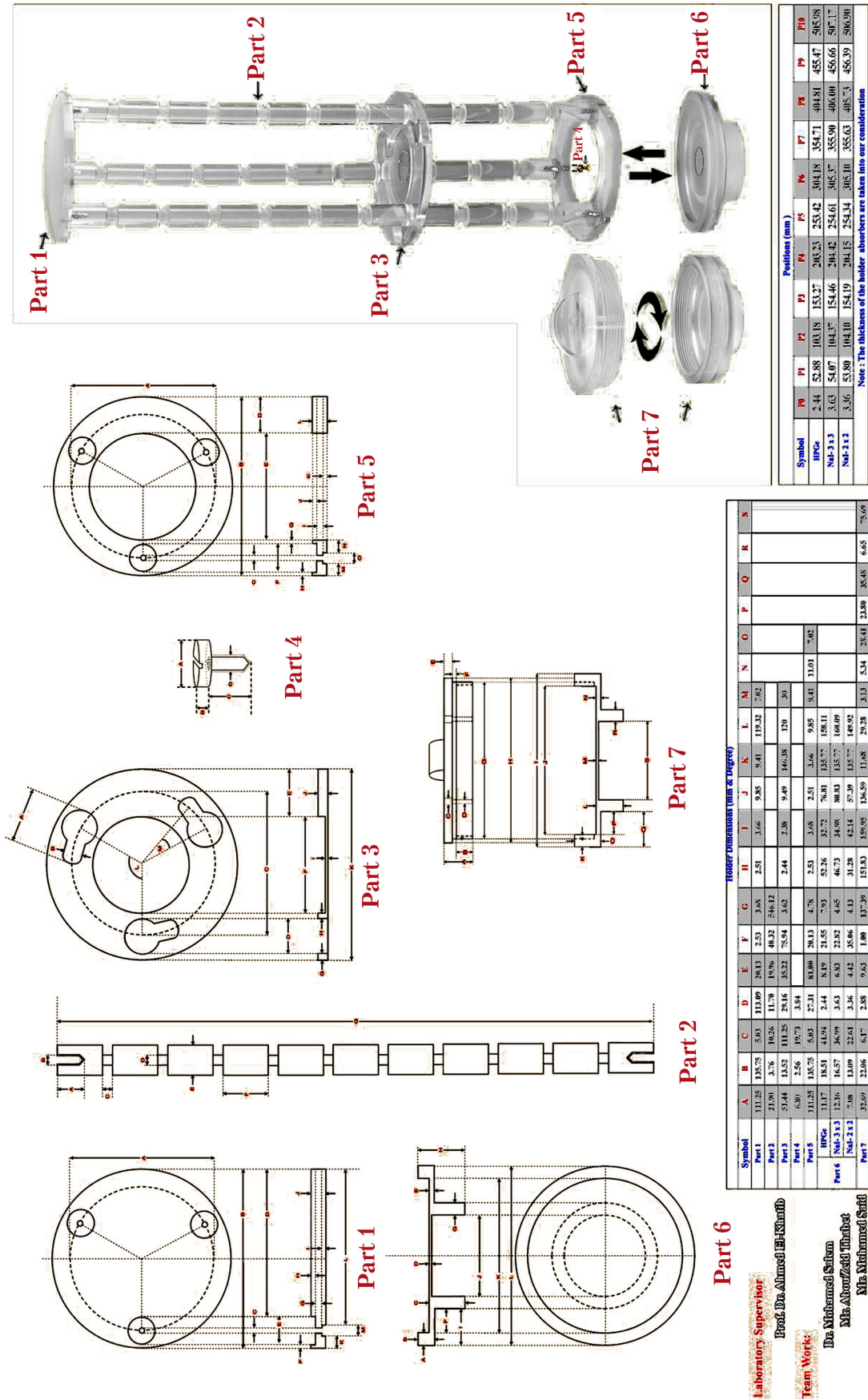


Figure 3 homemade Plexiglas holder parts drawing

curves with their associated uncertainties as a function of the photon energy for all calibration sources detectors listed in tables (5).

Results and Discussion

The comparison between Efficiency Transfer Theoretical Method (ETTM) and the experimental work, which is done at Younis. S. Selim Laboratory for Radiation Physics, Department of Physics, Faculty of Science, Alexandria University, was made in this part for different volumes of inverted well beakers (Marinelli beakers). This included study the effect of the source self -attenuation coefficient on the full-energy peak efficiency of HPGe detector and the percentage of errors between the measured and the calculated efficiencies(taking into account the effect of self- attenuation coefficient and with the neglecting effect of the self – attenuation coefficient) are shown in tables (6) and (7) respectively, which calculated from the formula:

$$\Delta\% = \frac{\epsilon_{\text{Cal}} - \epsilon_{\text{meas}}}{\epsilon_{\text{meas}}} \times 100 \quad (15)$$

where, ϵ_{cal} and, ϵ_{meas} , are the calculated and experimentally measured efficiencies, respectively.

The measured efficiency values as a function of the photon energy, $\epsilon(E)$, for HPGe sem-

iconductor detector was calculated with a dead time always less than 3% by:

$$\epsilon(E) = \frac{N(E)}{T \cdot A_s \cdot P(E)} \prod C_i \quad (16)$$

Where, $N(E)$, is the number of counts in the full-energy peak which can be obtained using Genie 2000 software, T , is the measuring time (in second), $P(E)$, is the photon emission probability at energy, A_s , is the radionuclide activity and, C_i , are the correction factors due to dead time, radionuclide decay.

The statistical uncertainties of the net peak areas were smaller than 1.0 % since the acquisition time was long enough to get the number of counts more than 10,000 counts. The background subtraction was done. The decay correction, C_d , for the calibration source from the reference time to the run time was given by:

$$C_d = e^{\lambda \cdot \Delta T} \quad (17)$$

Where, λ , is the decay constant and, ΔT , is the time interval over which the source decays corresponding to the run time.

The main source of uncertainty in the efficiency calculations was the uncertainties of the activities of the standard source solutions. Co-

Table (3) Half- lives, photon energies and photon emission probabilities per decay for the radionuclides used in this work

PTB-Nuclide	Energy (keV)	Emission Probability %	Half Life (Days)
¹⁵² Eu	121.78	28.40	4943.29
	244.69	7.49	
	344.28	26.60	
	778.90	12.96	
	964.13	14.00	
	1408.01	20.87	

Table (4) Activities of the used sources and their uncertainties

Source	Nuclide	Activity (kBq)	Reference Date 00:00 Hr	Uncertainty (%)
Point		290.0	1 June 2009	
M1	¹⁵² Eu	5	1 Jan 2010	□ 1.98
M2		5	1 Jan 2010	
M3		10	1 Jan 2010	

Table (5) Dimensions of the inverted well beaker sources.

inverted well beaker	Maximum volume(liter)	Maximum diameter(cm)	Minimum well diameter(cm)	Height of well(cm)
M1	0.5	11.70	7.70	6.80
M2	0.2	11.36	7.77	3.81
M3	1.0	14.00	8.50	6.10

incidence summing effects were negligible in the reference measurement geometries.

The uncertainty in the full-energy peak efficiency, σ_ϵ , was given by:

$$\sigma_\epsilon = \epsilon \cdot \sqrt{\left(\frac{\partial \epsilon}{\partial A}\right)^2 \cdot \sigma_A^2 + \left(\frac{\partial \epsilon}{\partial P}\right)^2 \cdot \sigma_P^2 + \left(\frac{\partial \epsilon}{\partial N}\right)^2 \cdot \sigma_N^2} \quad (18)$$

Where, σ_A , σ_P , and, σ_N , are the uncertainties associated with the quantities, A_S , $P(E)$, and, $N(E)$, respectively, assuming that the only correction made is due to the source activity decay.

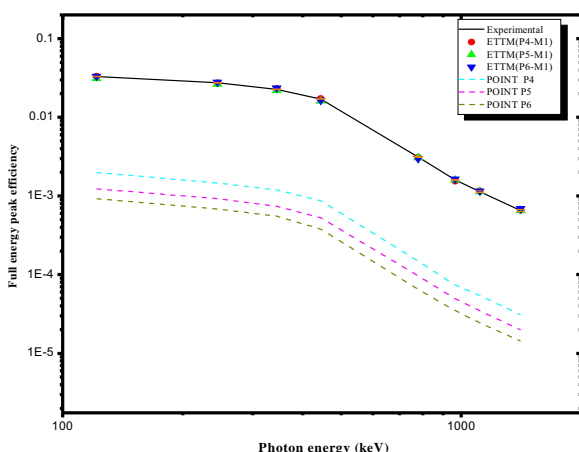
Obviously from figure (4) up to figure (9) that, the efficiency of the detector is higher at low source energies (absorption coefficient is very high) and decreases as the energy increases

Table (6) The percentage of error $\Delta\%$ between the efficiency results calculated by using ETTM for M1, M2 and M3 based on reference point source placed at positions P4=20 cm, P5=25 cm and P6=30 cm from the detector surface (taking into account the effect of self-attenuation coefficient) and the measured one

P4-M1	P5-M1	P6-M1	P4-M2	P5-M2	P6-M2	P4-M3	P5-M3	P6-M3
0	6	0	-1	4	6	0	5	-1
0	4	-2	3	7	9	-1	3	-3
-2	3	-4	3	7	8	-1	4	-4
0	6	3	0	6	11	-1	6	3
2	2	4	-5	-4	6	-1	0	1
3	0	-3	2	0	4	1	-1	-5
-2	0	-2	-4	-2	4	-1	1	-1
-1	0	-6	1	3	5	-3	-1	-7

Table (7) The percentage of error $\Delta\%$ between the efficiency results calculated by using ETTM for M1, M2 and M3 based on reference point source placed at positions P4=20 cm, P5=25 cm and P6=30 cm from the detector surface (without taking into account the effect of self-attenuation coefficient) and the measured one

P4-M1	P5-M1	P6-M1	P4-M2	P5-M2	P6-M2	P4-M3	P5-M3	P6-M3
-67	-58	-68	-60	-51	-48	-168	-132	-140
-45	-40	-49	-33	-28	-26	-120	-89	-99
-42	-35	-46	-28	-22	-22	-117	-67	-74
-37	-27	-31	-29	-20	-14	-119	-66	-82
-26	-25	-23	-26	-25	-14	-37	-57	-71
-22	-25	-29	-15	-18	-13	-50	-50	-42
-26	-23	-26	-21	-18	-12	-31	-46	-57
-23	-21	-28	-12	-10	-8	-9	-34	-62



Figure(4) Comparison between the experimental and calculated (ETTM) efficiency of M1 based on conversion from point efficiency curve at position P4, P5 and P6 taking into account the effect of self-attenuation coefficient

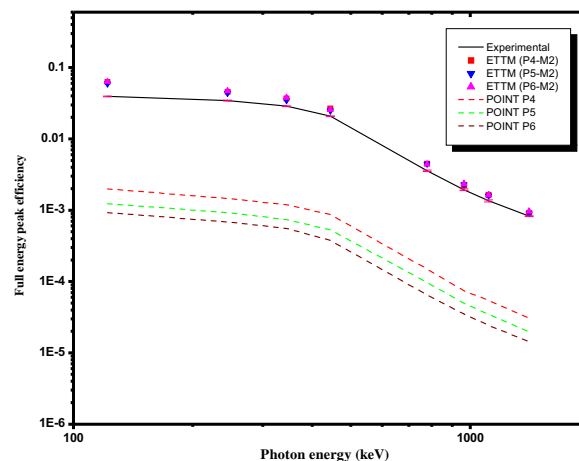


Figure (7) Comparison between the experimental and calculated (ETTM) efficiency of M2 based on conversion from point efficiency curve at position P4, P5 and P6 without taking into account the effect of self-attenuation coefficient

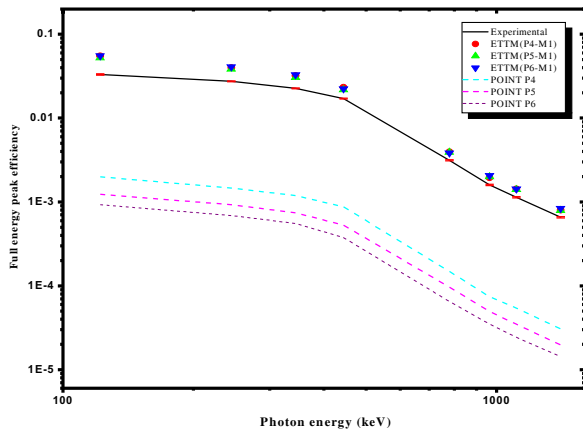


Figure (5) Comparison between the experimental and calculated (ETTM) efficiency of M1 based on conversion from point efficiency curve at position P4, P5 and P6 without taking into account the effect of self – attenuation coefficient

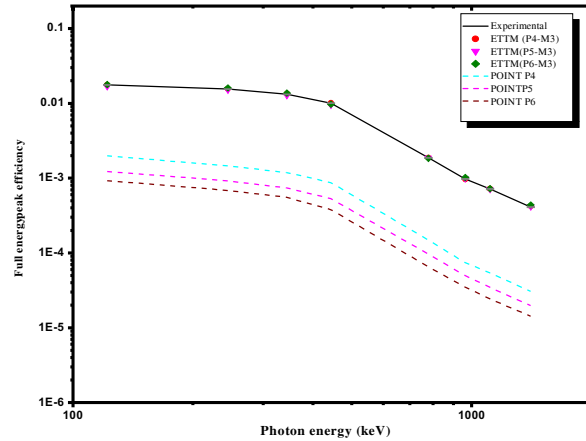
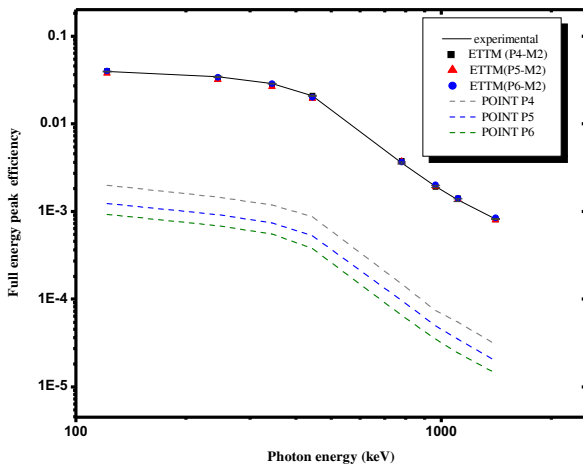


Figure (8) Comparison between the experimental and calculated (ETTM) efficiency of M3 based on conversion from point efficiency curve at position P4, P5 and P6 taking into account the effect of self – attenuation coefficient



Figure(6) Comparison between the experimental and calculated (ETTM) efficiency of M2 based on conversion from point efficiency curve at position P4, P5 and P6 taking into account the effect of self – attenuation coefficient

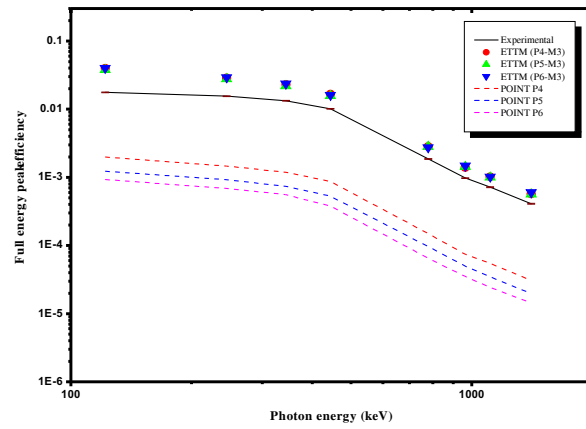


Figure (9) Comparison between the experimental and calculated (ETTM) efficiency of M3 based on conversion from point efficiency curve at position P4, P5 and P6 without taking into account the effect of self – attenuation coefficient

(fall off in the absorption coefficient) because the photoelectric is dominant below 100 keV. Also, it can be seen clearly the effect of the self– attenuation coefficients in the calculation of the detector efficiency.

Conclusion

This work done by using a simple (ETTM) to evaluate the full-energy peak efficiency over a wide energy range for inverted well beaker sources which based on measuring an axial

point source placed at different positions using p-type HPGe detector, one can conclude that there is a good agreement between the calculated efficiency and the experimental measurements done by using different volumes of the inverted well beakers.

Also, it is clearly observed from the results that the efficiency of the detector decreases when one includes the effect of the various attenuation coefficients of the contents of the used source matrix.

18.05.2013

Acknowledgment

The authors would like to express their sincere thanks to Prof. Dr. Mahmoud. I. Abbas, Faculty of Science, Alexandria University, for the very valuable professional guidance in the area of radiation physics and for his fruitful scientific collaborations on this topic.

Dr. Mohamed. S. Badawi would like to introduce a special thanks to The Physikalisch-Technische Bundesanstalt (PTB) in Braunschweig, Berlin, Germany for fruitful help in preparing the homemade volumetric sources.

Bibliography:

1. Selim, Y. S., Abbas, M. I., 1994. Source-detector geometrical efficiency, *Radiat. Phys. Chem.* 44, 1.
2. Selim, Y. S., Abbas, M. I., 1995. Direct calculation of the total efficiency of cylindrical scintillation detectors for non-axial point sources, *Egypt. J. Phys.* 26, 79.
3. Abbas, M. I., Selim, Y. S., Bassiouni, M., 2001. HPGe detector photopeak efficiency calculation including self-absorption and coincidence corrections for cylindrical sources using compact analytical expressions, *Radiat. Phys. Chem.* 61, 429.
4. Tim Vidmar, Branko Vodenik, Marijan Necemer (2010) «Efficiency transfer between extended sources» *Applied Radiation and Isotopes* 68 (2010) 2352–2354
5. Le`py, M. C., Altizoglou, T., Arnold, D., et al., 2001. Intercomparison of efficiency transfer software for gamma-ray spectrometry. *Appl. Radiat. Isot.* 55(4), 493–503.
6. Vidmar, T., Aubineau Laniece, I., Anagnostakis, M. J., et al., 2008. An intercomparison of Monte Carlo codes used in gamma-ray spectrometry. *Appl. Radiat. Isot.* 66 (6–7), 764–768.
7. Piton, F., Lepy, M. C., Be, M. M., Plagnard, J., 2000. Efficiency transfer and coincidence summing corrections for gamma-ray spectrometry, *Appl. Radiat. Isot.* 52, 791.
8. Jovanovic, S., Dlabac, A., Mihaljevic, N., Vukotic, P., 1997. ANGLE: A PC-code for semiconductor detector efficiency calculations, *Radiat. Phys. Chem.* 218, 13.
9. Badawi, M. S., (2009). PhD. Thesis, Faculty of Science, Alexandria University, Egypt.
10. Mahmoud I. Abbas, «HPGe detector absolute full-energy peak efficiency calibration including coincidence correction for circular disc sources» *J. Phys. D: Appl. Phys.* 39 (2006) 3952–3958.
11. Sherif S. Nafee, Mohamed S. Badawi, Ali M. Abdel-Moneim, Seham A. Mahmoud. «Calibration of the 4p r-ray spectrometer using a new numerical simulation approach» *Applied Radiation and Isotopes* 68 (2010) 1746–1753
12. Debertin, K., and Schotzig, U., 1979. Coincidence summing corrections in Ge(Li)-spectrometry at low source-to-detector distances, *Nucl. Instrum. Meth.* A158, 471.

M. S. Badawi*, Physics Department, Faculty of Science, Alexandria University, 21511 Alexandria, Egypt.
[Doctor], e-mail: ms241178@hotmail.com, Tel: +201005154976.

S. S. Nafee, Physics Department, Faculty of Science, Alexandria University, 21511 Alexandria, Egypt.
[Doctor], e-mail: nafee_shra@yahoo.com, Tel: +201010058780.

S. M. Diab, Physics Department, Faculty of Science, Alexandria University, 21511 Alexandria, Egypt.
[Assistance Lecturer], e-mail: samahdiab_diab@yahoo.com, Tel: +201006883758.

A. M. El-Khatib, Physics Department, Faculty of Science, Alexandria University, 21511 Alexandria, Egypt.
[Professor. Doctor], e-mail: Elkhatib60@yahoo.com, Tel: +201000230122.

E. A. El-Mallah, Physics Department, Faculty of Science, Alexandria University, 21511 Alexandria, Egypt.
[Doctor], e-mail: ekramelmallah@yahoo.com, Tel: +201005154976.

* Corresponding author at: Cell: +201005154976

E-mail addresses: ms241178@hotmail.com (M. S. Badawi).